Neuron 50, 937–949, June 15, 2006 ©2006 Elsevier Inc. DOI 10.1016/j.neuron.2006.03.021

Representation of Natural Stimuli in the Rodent Main Olfactory Bulb

Da Yu Lin,[1,*] Stephen D. Shea,[1] and Lawrence C. Katz[1,2]
[1] Howard Hughes Medical Institute and Department of Neurobiology
Box 3209
Duke University Medical Center
Durham, North Carolina 27710

Summary

Natural odorants are complex mixtures of diverse chemical compounds. Monomolecular odorants are represented in the main olfactory bulb by distinct spatial patterns of activated glomeruli. However, it remains unclear how individual compounds contribute to population representations of natural stimuli, which appear to be unexpectedly sparse. We combined gas chromatography and intrinsic signal imaging to visualize glomerular responses to natural stimuli and their fractionated components. While whole stimuli activated up to 20 visible glomeruli, each fractionated component activated only one or few glomeruli, and most glomeruli were activated by only one component. Thus, responses to complex mixtures reflected activation by multiple components, with each contributing only a small part of the overall representation. We conclude that the population response to a complex stimulus is largely the sum of the responses to its individual components, and activation of an individual glomerulus independently signals the presence of a specific component.

Introduction

Many organisms rely heavily on their olfactory system to identify food sources, judge the social status of conspecifics, and avoid predators. The odorants that give rise to these behaviors are complex mixtures of chemicals that must be represented as distinct patterns of activity by neurons in the olfactory system. The fundamental principles that underlie the encoding and discrimination of naturally occurring odor stimuli remain unclear, even within the main olfactory bulb (MOB), which is the first stage in the neural processing of volatile odorants.

The outer layer of the MOB comprises thousands of glomeruli, spherical regions of neuropil formed by an aggregation of axons from olfactory receptor neurons (ORN) expressing the same olfactory receptor (OR) (out of ~1000) (Buck and Axel, 1991; Mombaerts et al., 1996). Each glomerulus serves as a point of contact between ORN axons and the dendrites of an exclusive set of mitral/tufted cells, which are the principal output neurons of the MOB. The segregation of sets of functionally coherent inputs and their postsynaptic targets into discrete glomeruli delineates a mechanism for spatial coding of odors across the MOB neural population. The response characteristics of a glomerulus are defined by its OR (Bozza et al., 2002) and appear to be uniform (Wachowiak et al., 2004), thus the glomeruli are the functional units of this spatial code.

Numerous studies have capitalized on this structural aspect of the mammalian MOB, visualizing patterns of glomerular activity with a wide range of anatomical (e.g., Guthrie et al., 1993; Johnson et al., 2002) and imaging techniques (e.g., Yang et al., 1998; Rubin and Katz, 1999; Wachowiak and Cohen, 2001; Spors and Grinvald, 2002; Bozza et al., 2004). This body of literature generally shows that individual odors activate distinct patterns of glomeruli that are relatively symmetric between bulbs and roughly stereotyped between animals, but that often expand dramatically with increasing concentration. The sometimes extensive patterns of activated glomeruli seen in response to a monomolecular odor suggest that natural odors composed of dozens of distinct volatiles could activate large expanses of the MOB. Yet, studies that visualized responses to natural stimuli showed activity patterns that did not appear to be more extensive than those seen with monomolecular chemicals at relatively high concentrations (e.g., Rubin and Katz, 1999; Schaefer et al., 2001; Takahashi et al., 2004b). Therefore it remains unclear how individual chemicals in the context of a complex natural stimulus are represented at the glomerular level. Component concentrations are dictated by the properties of the stimulus and many are quite low; thus, it is possible that the response to such stimuli is largely determined by a small number of perceptually dominant compounds.

It is also unclear whether or not the representations of natural stimuli reflect mutual interactions among their components. Inhibitory connections in the MOB circuit may support "lateral inhibition" in the glomerular layer via short axon cells (Aungst et al., 2003) and among mitral cells via granule cells (Yokoi et al., 1995; Urban, 2002). Previous studies that imaged glomerular responses to binary mixtures found that these responses were predicted by a linear sum of responses to the components, suggesting little interaction between their representations (Belluscio and Katz, 2001; Tabor et al., 2004; McGann et al., 2005), although this was not true in recordings from mitral cells (Tabor et al., 2004). Nonetheless, the complexity of most natural stimuli raises the possibility of far more extensive interactions.

We used intrinsic signal imaging of MOB glomeruli to visualize population responses to a wide range of complex odorants derived from natural sources, including foodstuffs, nesting materials, rodent attractants and repellents, and urine from predators. Then, by combining this technique with gas chromatography (GC), we sequentially examined the responses to individual stimulus components and compared them with responses to their parent stimuli. The data show that (1) each stimulus component typically activates only a small fraction of the glomeruli that contribute to the whole stimulus representation, (2) glomerular responses to natural odorants are highly specific, and (3) the glomerular

*Correspondence: dayulin@neuro.duke.edu
[2] Deceased.

Table 1. Natural Stimuli Activating Glomeruli on the Dorsal Surface of the MOB

None			Weak	Strong
mouse urine	wheat bread	honey	hay	cloves
mouse feces	peanuts	beer	wine	fox urine
rat urine	millet seeds	tomato	cake	tea
chocolate	sesame seeds	coconut	bobcat urine	coffee
mint	groats	ginger	peanut butter	burnt hay
anise	yogurt	mango	sesame oil	liquid smoke
vanilla	butter	basil	onion	cumin
hot pepper	buttermilk	rosemary	garlic	cardamom
apple	cheese	black pepper	banana	nutmeg
orange	jam	cinnamon	roasted almonds	
strawberry	corn chips	mushroom	vinegar	
grape	blue cheese	oregano	rice wine	
		rose	soy sauce	
			tobacco	

Thirty-seven natural stimuli were tested that evoked no glomerular activation on the dorsal surface of the MOB. Weak stimuli activated one to five dorsal glomeruli. Strong stimuli activated more than five glomeruli strongly.

representations of complex natural stimuli are well predicted by the sum of the responses to their molecular constituents.

Results

Spatially Unique Responses to Natural Stimuli

Intrinsic signal imaging has been widely used to observe the responses of individual glomeruli on the dorsal surface of the MOB (Rubin and Katz, 1999; Uchida et al., 2000; Belluscio and Katz, 2001; Meister and Bonhoeffer, 2001) (see Experimental Procedures). About 200 glomeruli could be visualized in one bulb by thinning the bone covering its dorsal surface.

Among the 60 diverse natural stimuli we tested, 14 evoked weak activity (1 to 5 glomeruli) and 9 evoked strong activity (>5 glomeruli); the singly activated glomeruli were in characteristic locations and the multiple glomeruli formed unique patterns (Table 1). Seasonings such as cardamom, clove, cumin, nutmeg, and garlic activated multiple glomeruli as reported previously (Takahashi et al., 2004b) (Figures 1B–1D). Fermented products such as vinegar and soy sauce activated several partially overlapping anterior glomeruli. Coffee evoked responses in more than ten glomeruli arranged in one anterior and one posterior cluster (Figure 1E). Although hay generated no response, burnt hay elicited widespread glomerular activity throughout the dorsal surface (Figure 1F). Roasted almonds, peanut butter, and sesame oil activated three to four similar glomeruli located in the anterior portion of the bulb (Figures 1G and 1H). No glomeruli visible on the dorsal surface were activated by mouse urine, a finding that is consistent with electrophysiology, imaging, and *c-fos* results in previous studies (Schaefer et al., 2001; Lin et al., 2005) (Figure 1K). Urine from two common mouse predators, bobcat and red fox, strongly activated several glomeruli each (Figures 1I and 1J). A number of fruits (with the exception of banana), herbs, grains, and diary products failed to consistently elicit responses.

Activated glomeruli varied in size (from 50–200 μm in diameter), which likely reflects differences in both anatomy and response intensity (Royet et al., 1988). Different natural stimuli belonging to the same category (e.g., fruits, spices, etc.) often appeared to activate comparable numbers of glomeruli on the dorsal surface; this could be due to similar chemical compositions resulting from common metabolic pathways or processing procedures. For instance, according to our mass spectrum (MS) analysis, fruits generally contain many esters, while long carbon chain alkanes and alkenes are commonly found in grains. Figure 1M shows the overlaid response patterns from all nine effective stimuli (Figures 1B–1J). Fifty distinct glomeruli were activated across all stimuli. Among those glomeruli, 74% (37/50) responded to only one stimulus, 18% (9/50) were activated two to four times, and the remaining 8% (4/50) were activated by most stimuli (Figure 1N). The latter activations were due to specific responses to two mixture components that were nearly ubiquitous in our stimulus set (see below).

Glomerular activations showed variable time courses (Figure S1 in the Supplemental Data). While most glomeruli were activated within 1 s of odor onset as previously reported (Meister and Bonhoeffer, 2001), some responses reached their maximum intensity at different rates. Similar phenomena have been reported in imaging studies using calcium indicators and voltage-sensitive dyes (Wachowiak and Cohen, 2001; Spors and Grinvald, 2002). Among the 50 glomeruli shown in Figure 1N, 27 reached their peak intensity before odor offset (odor was delivered for 5 s) and 17 reached their maximum response within 10 s of odor offset. Notably, the remaining six glomeruli continued to increase their response strength for more than 10 s following odor offset. Most (5/6) of those slow-response glomeruli were located in the posterior portion of the MOB. These observed differences in time course were not related to response intensity (Figure S1D, $r^2 = 0.006$, $p = 0.59$), but instead may reflect the chemical properties of ligands. In subsequent experiments with gas chromatography, we noticed that posterior glomeruli were often activated by compounds with long retention times, indicative of a high molecular weight.

Responses to Individual Components in Natural Stimuli

Natural stimuli evoked responses that were complex and distinct but also remarkably sparse, activating at most 20% of the visible dorsal surface glomeruli despite

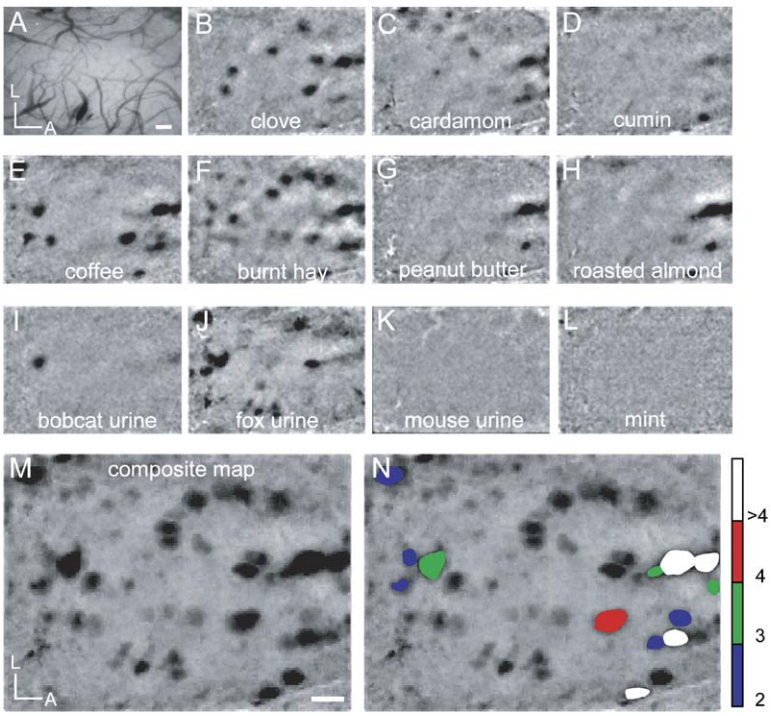

Figure 1. Population Representations of Natural Odorants

(A) Blood vessel pattern overlying the imaged region visualized through thinned bone. Scale bar, 200 μm. L, lateral; A, anterior.

(B–L) Intrinsic signal image response evoked by clove (B), cardamom (C), cumin (D), coffee (E), burnt hay (F), peanut butter (G), roasted almonds (H), bobcat urine (I), fox urine (J), mouse urine (K), and mint (L).

(M) Composite map of all responses in (B)–(J) showing 50 activated glomeruli.

(N) Glomeruli activated by multiple stimuli. Blue glomeruli were activated by two different stimuli; green glomeruli were activated by three stimuli; red glomeruli were activated by four stimuli; white glomeruli were activated by more than four stimuli; all other glomeruli were uniquely activated by a single stimulus.

containing dozens of volatile chemicals. In order to understand how each chemical contributes to these responses, we combined GC and intrinsic signal imaging (GC-I) to visualize MOB activation in response to sequentially delivered, fractionated odorant components (Figure S2). It is possible that one or a few dominant volatile components present in the stimulus each activates many glomeruli, or that many distinct volatiles each activates one or a few glomeruli.

Three highly effective natural stimuli (cumin, coffee, and clove) were chosen for detailed analysis. The response pattern for each natural stimulus was grossly similar between individual animals as observed before (Belluscio and Katz, 2001) (Figure S3). During GC presentation of the sequentially-eluted volatiles of each stimulus, a characteristic series of glomeruli were activated at distinct time points. Activations were observed throughout the GC runs for all three stimuli. A typical response lasted from 6 to 60 s, during which one or a few glomeruli abruptly appeared and then disappeared gradually (Figures 2B and 2C) (Movie S1). The most intense responses (Z score ≤ -3, see Experimental Procedures) were very consistent between trials, while weaker responses were less repeatable. Signals from at least three identical GC trials in the same animal were averaged to produce one usable dataset. In total, seven data sets were collected from four animals for coffee, nine datasets from seven animals for cumin, and 11 datasets from seven animals for clove. Consistent with mitral cell responses during GC elution of urine, the size of flame ionization detector (FID) peaks and the magnitude of glomerular responses were unrelated (Lin et al., 2005). It is well known from GC-olfactometry (GC-O) experiments with human subjects that the perceived potency of an odorant is independent of peak size, owing to differences in psychophysical thresholds (van Ruth, 2001).

Glomerular responses to the separated components of natural stimuli were highly specific. More than 100 chemicals were presented during each GC run as determined by mass spectrum detector (MSD) and FID. Nonetheless, only a small fraction of all visible glomeruli were activated, and 72% (398/556) of the activated glomeruli responded at a single time point. Among the remaining activated glomeruli, 23% (129/556) were activated twice and 5% (29/556) responded at three or four different times (Figures 3A and 3B).

We were also able to assess the sparseness of population representations by quantifying the extent of responses to components eluted at any given time point. In our GC-I data sets, 464 glomerular responses were observed; glomeruli activated within a time window of 2 s are considered to be part of the same response. In 66% (304/464) of glomerular responses, each corresponding to a small fraction of the mixture, only one dorsally visible glomerulus was activated. Twenty percent (93/464) of responses involved two glomeruli, 7% (34/464) involved three glomeruli, and the remaining 7% (33/464) included four to eight glomeruli (Figures 3C and 3D). Responses engaging multiple glomeruli may be overestimated due to coelution of multiple components; time constraints necessitated the use of relatively short GC programs (20 min) which somewhat decreased the temporal resolution of the GC.

The spatial locations of activated glomeruli were unaffected by changing the order in which the stimulus components were delivered. BP-5 GC columns separate chemicals according to their molecular masses and boiling points while BP-20 columns separate based on polarity. Therefore, stimulus components will elute in a different order from each type of column. In five experiments (two from coffee, three from cumin), data sets collected using BP-5 and BP-20 columns were directly

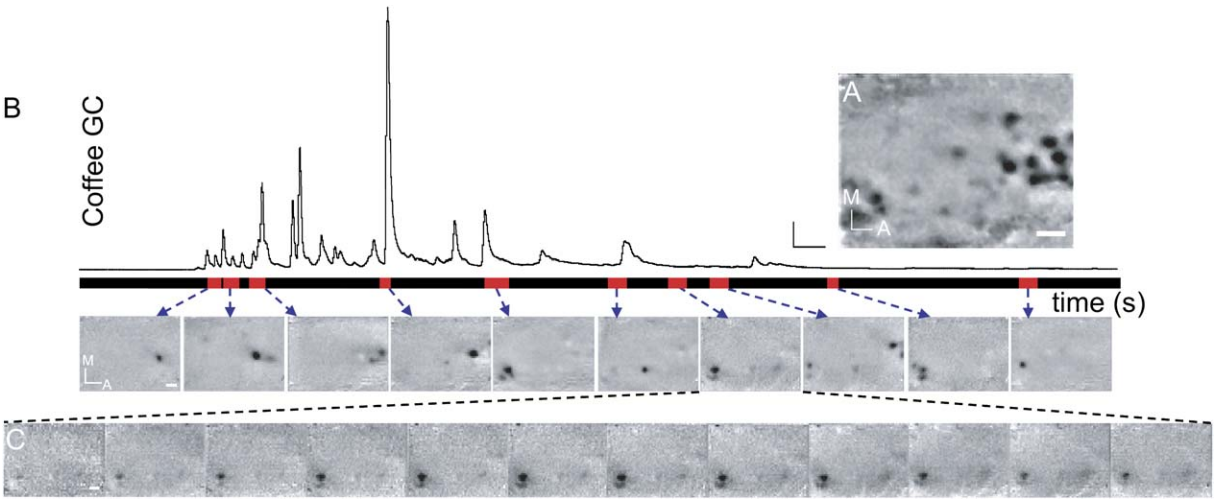

Figure 2. Sequential Glomerular Activation during GC Separation of Natural Stimulus Components

(A) Response to whole coffee. Scale bar = 200 μm. M, medial; A, anterior.

(B) A series of images (lower panel) showing responses (averaged over several frames) at different time points during the elution of coffee volatiles from the GC (FID signal, upper panel). The red bars denote the periods contributing to each image. Upper panel scale bar = 100 mV / 25 s; lower panel scale bar = 200 μm. M, medial; A, anterior.

(C) A set of frames (1 frame/s) showing one glomerular response in greater temporal detail.

compared. In total, 111 and 104 glomeruli were activated during GC runs using BP-5 and BP-20 columns, respectively, and 92 glomeruli were activated during both. Strongly activated glomeruli were more reliably activated by both columns. Considering only highly active glomeruli (Z score ≤ -3), 39/43 glomeruli activated during BP-5 GC runs were present in BP-20 GC runs. All 46 strongly activated glomeruli during BP-20 GC runs were also active when using a BP-5 column. Use of these two columns influences elution order, not chemical composition, so discordant glomeruli over the course of our experiments may reflect biological response variation.

Since the goal of this study is to compare responses to individual components and to natural stimuli and elucidate their underlying relationship, we sought methods for concentrating stimulus volatiles while retaining their natural ratios as faithfully as possible. Two independent methods, solid phase microextraction (SPME) fiber adsorption and cryotrap, were used to minimize methodology-related biases in volatile collection. With short periods of exposure, SPME fibers concentrate chemicals from the odor headspace (but minimally from the liquid or solid phases) through adsorption (Roberts et al., 2000). Because cryotrap relies only on condensation from the vapor phase, this technique concentrates the odor headspace with the least bias. Similar GC profiles were obtained using these two methods (cross correlation = 0.75 ± 0.05 compared with 0.92 ± 0.06 for GC profiles obtained using the same concentrating methods, n = 3) (Figure S4). While SPME fibers slightly favor volatiles with higher molecular weight (MW > 120), cryotrap retains compounds with very low molecular mass (MW < 60) more efficiently.

The activation patterns were fairly consistent between the two concentrating approaches, suggesting that biases related to methodology were minimized. In four experiments (one coffee, one clove, and two cumin), we compared the GC-I results obtained with SPME and cryotrap. One hundred twenty-seven glomeruli were activated using cryotrap and 119 glomeruli were activated using a SPME fiber; 89 of these glomeruli were activated under both conditions. As before, strongly activated glomeruli showed much better agreement between methods. With cryotrap, 32/35 glomeruli with Z score ≤ -3 were also found for the same stimulus using the SPME approach. For SPME fibers, 25/26 strongly activated glomeruli were also active during cryotrap GC runs.

Sensitive and Specific Glomerular Responses

The activation of individual glomeruli by only one or a few components out of more than 100 suggests that glomerular activities are quite narrowly tuned at this concentration range, at least within dorsally visible regions. The accuracy of this conjecture is difficult to evaluate as long as the identity of most ligands in the stimuli are unknown. MSD uses molecular fragmentation patterns (mass spectra) to deduce the structure of unknown compounds. Combining GC-I with an MSD allowed us to identify specific ligands in our stimuli that are responsible for activating dorsally visible glomeruli. Due to the frequent ambiguity of mass spectra and the limited commercial availability of ligands, we could only definitively identify a fraction of the components. When we did identify a ligand, GC peaks were first selected on the basis of timing; we focused on peaks that eluted <10 s prior to the onset of a glomerular response. Then, candidate chemicals were identified based on their fragmentation patterns. Finally, we confirmed the chemical structure of a ligand by verifying an identical glomerular response to the pure compound. For example, coffee activated a distinct pattern of glomeruli. One glomerulus was activated at 304 s in the GC run, and the mass spectrum of the immediately preceding peak suggested that the compound was 2-methyl 2-butenal (2MBE). Presentation of diluted

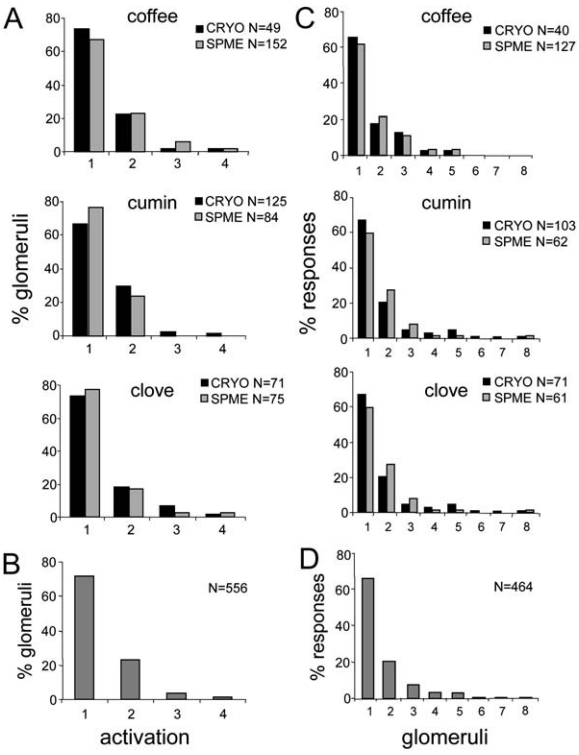

Figure 3. Sparse Representations of Individual Components and Specific Glomerular Responses

(A) Histograms showing the distributions of number of activations per glomerulus during GC runs using coffee (49 and 152 glomeruli from one cryo and four SPME experiments, respectively), cumin (125 and 84 glomeruli from five cryo and four SPME experiments, respectively), and clove (71 and 75 glomeruli from four cryo and five SPME experiments, respectively). Black bars indicate data collected using the cryotrap-GC method; gray bars show data obtained using the SPME-GC method.

(B) Histogram of the data in (A) collapsed over all GC conditions and stimuli.

(C) Histograms showing the distributions of number of glomeruli per activation during GC runs using coffee, cumin, and clove. Color conventions as in (A).

(D) Histogram of the data in (C) collapsed over all GC conditions and stimuli.

pure 2MBE with an olfactometer exclusively activated the identified glomerulus. Similar mass spectrum analysis identified eugenol (EG) in clove, 3-p-Menthen-7-al (3MT) in cumin, and 3-methyl butanal (3MB) and 2-methyl butanal (2MB) in all three stimuli. With the exception of 3MT, their identities were also confirmed by presenting commercially available pure compounds.

EG is present at high levels (>1000 ppm) in clove and has been reported to activate glomeruli on the dorsal surface in previous studies (Takahashi et al., 2004b). 3MT is a key contributor to cumin's characteristic smell. It was identified as a candidate ligand based on its mass spectra and retention times on both BP-5 and BP-20 columns. Several structurally and perceptually similar chemicals (Cuminaldehyde, 1,3-p-Menthadien-7-al, and 4-p-Menthadien-7-al) are also present in cumin at comparable or higher concentrations (Tassan and Russell, 1975), but only 3MT elicits responses (Z score ≤ -2) from the identified glomerulus. These observations suggest that the selectivity of glomerular responses was not necessarily due to a lack of structurally related chemicals in a stimulus and may truly reflect narrow tuning properties. Indeed, 2MB, 3MB, and 2MBE are themselves structurally similar, yet they activated distinct glomeruli (Figure 4D). We determined response thresholds and dosage response curves for 2MB, 3MB, and 2MBE (Z score ≤ -2). 3MB activated glomeruli at <100 ppb at the nose, while response thresholds for 2MB and 2MBE were <10 ppb at the nose (Figures S5A–S5C).

Some glomeruli were activated by multiple natural stimuli (Figure 1N). As shown in Figures 5A and 5B, two glomeruli (red arrow and blue arrow) were excited by both clove and coffee. However, GC data indicate that for both stimuli, the glomerulus marked by the red arrow was activated by 2MB, which eluted at identical retention times (230–236 s) in clove and coffee GC runs (Figures 5C and 5D). The glomerulus marked by the blue arrow was activated by two structurally similar compounds (ethyl tiglate and 2MBE) (Figures 5C and 5D). Although not all ligands activating a glomerulus can be identified, these results suggest that a common glomerular response to different natural stimuli might simply reflect the shared presence of identical or structurally similar ligands rather than coarse tuning of the glomerulus.

To further evaluate the specificity of glomerular responses, we tested 29 chemicals with structures similar to 2MB, 3MB, and 2MBE at concentrations of 10^{-5} (v/v) (Figure 4). Each of the 29 chemicals can be obtained by modifying a single functional group on one of those three known ligands. Four chemicals (butanal, 2-methyl pentanal, 2-methyl propanal, and 2-Methyl-butyric acid methyl ester) activated the glomerulus (activation is defined as Z score < -2) that showed the strongest response to 2MB (red circle in Figure 4A). Butanal was the only compound that activated the 3MB responsive glomerulus (blue circle in Figure 4B). 2-methyl pentenal, methyl tiglate, and ethyl tiglate evoked responses from the glomerulus activated by 2MBE (green circle in Figure 4C). In many cases, subtle changes in chemical structures altered the glomerular responses significantly. For example, while methyl tiglate strongly activated the glomerulus, its *cis* isomer, methyl angelate, failed to generate a response. In another example, 2-methyl pentenal activated the 2MBE responsive glomerulus, while 2-methyl propenal did not, instead activating an immediately adjacent glomerulus (Figure 4C). The results indicate that these glomerular responses are highly specific, usually requiring the presence of several molecular features and the absence of others.

The Response to a Complex Stimulus Closely Matches the Cumulative Response to Its Individual Components

In order to understand the relationship of the response to a mixture with the response to its parts, we compared the activation patterns seen for each stimulus to the cumulative response to its fractionated volatiles. One possibility is that extensive interactions among the responsive glomeruli prevent the prediction of the response to a stimulus from the responses to its components. On the contrary, however, we found that the response to a natural stimulus closely matches a linear summation of the responses to its monomolecular elements.

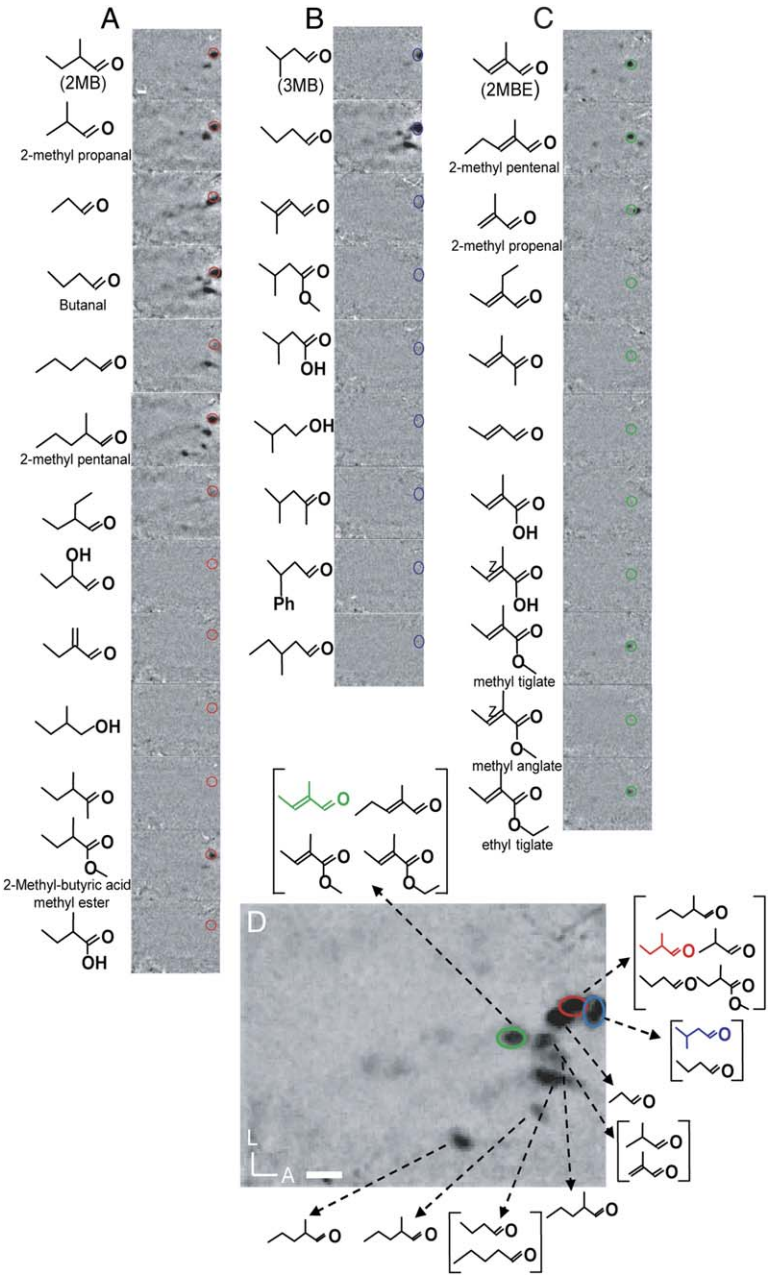

Figure 4. Glomerular Receptive Fields

(A) Intrinsic signal response to 2MB and 12 structurally similar compounds. The glomerulus primarily responding to 2MB is circled in red.

(B) Response to 3MB and eight structurally similar compounds. The 3MB-sensitive glomerulus is circled in blue.

(C) Response to 2MBE and ten structurally similar compounds. The 2MBE-sensitive glomerulus is circled in green.

(D) A composite map showing all responses elicited by the chemicals in (A) through (C), with colored circles designating the 2MB, 3MB, and 2MBE glomeruli. Arrows indicate ligands that activate each glomerulus (Z score ≤ -2). Both scale bars in (A) and (D) indicate 200 μm.

Indeed, in one exceptional experiment using clove as a stimulus, glomerular activation was seen at three time points in the GC run (Figures 6A and 6B), and all three compounds associated with these activations were identified (Figure 6A). We then replicated the response to whole clove using a mixture containing those three compounds at concentrations estimated from GC data (Figures 6D and 6E). Comparison of the mixture and component responses to the clove response showed excellent overlap (Figures 6F and 6G). Our finding that the activation pattern of a natural mixture containing hundreds of chemicals can be effectively reconstituted (at least within the imageable area) using a simple mixture suggests that responses to individual components might be largely independent and additive at the glomerular level.

In most cases, the glomerular responses during GC runs are far more complex. On average, 36 ± 10 responses were observed during a coffee GC run. With such a large number of responses, it was impossible to identify the structures of all ligands. We therefore developed a quantitative method to compare the degree of similarity (matching quality) between response maps for the same stimulus acquired under intact and GC-fractionated conditions (Figure 7). Briefly, an automated detection algorithm was used to identify active pixel clusters (corresponding to glomeruli) during GC runs. The position and intensity of these glomeruli were compared to those of the glomeruli identified in the intact map and were used to calculate a matching quality score (see Experimental Procedures). On average, the matching quality between the two conditions for the same animal was

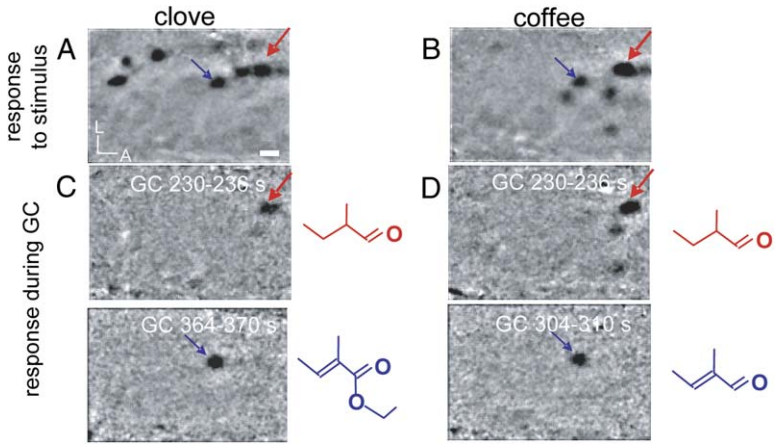

Figure 5. Glomeruli Activated by Shared Components in Different Stimuli

(A) Response to whole clove. Red and blue arrows indicate glomeruli also activated by coffee. Scale bar = 200 μm. L, lateral; A, anterior.

(B) Response to whole coffee. The glomeruli shared with clove are marked.

(C and D) Responses to GC elution of clove (C) and coffee (D) at two time points. Panels depict the average of frames collected during two windows of time corresponding to activation of the glomeruli marked by arrows in (A) and (B). In each case, the chemical structure specified by the mass spectrum at that time point is shown on the right. Note that the glomerulus marked by the red arrow was activated by the same compound in both stimuli (2MB). The glomerulus marked by the blue arrow was activated by two structurally similar compounds (ethyl tiglate in clove and 2MBE in coffee).

80.2% ± 9.9%. In contrast, matching quality was lower than 15% when intact and fractionated maps were from different stimuli (Figure S6). Coffee generated the most complex activation patterns and showed the highest matching quality (83.4% ± 3.6%). Cumin and clove had matching qualities of 72.2% ± 12.7% and 83.3% ± 10.5%, respectively. Different concentrating methods yielded similar matching qualities (cryotrap: 76.4% ± 12.5%, SPME: 83.4% ± 6.0%; unpaired t test, $p = 0.08$).

While the matching quality was generally high, there were still some glomeruli that were not observed in response to both complete and fractionated stimuli. Some of these mismatches could be explained by concentration differences between the two odor delivery conditions. However, for the following reasons this is unlikely to be the main source of variance. First, concentration differences were minimized by injecting exactly the same amount of odor headspace into the GC as was presented by the olfactometer. Second, there was no obvious relationship between activation intensity and the likelihood of a glomerular match, contradictory to what one would expect if concentration differences were the principal source of variation. Among weakly activated glomeruli (Z score > −3) 23% (92/404) were mismatched, which was comparable to the 19% (48/248) mismatch for strongly activated glomeruli (Z score ≤ −3).

Most (80%) of the discrepancy between maps was due to the appearance of new strongly activated glomeruli in the GC condition that were not observed for the whole stimulus. Most such glomeruli were consistently

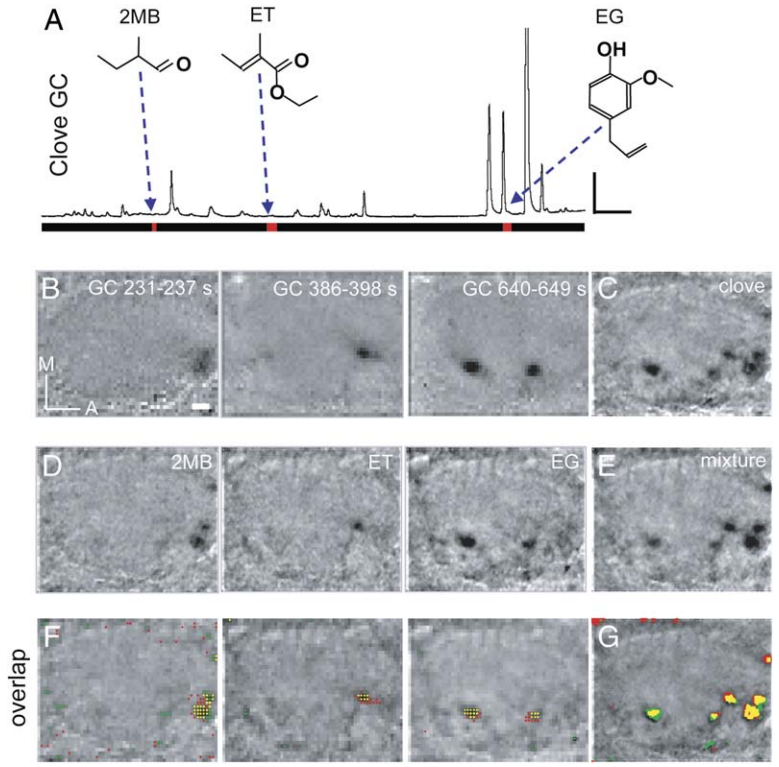

Figure 6. Replication of the Response to Whole Clove with a Simple Mixture

(A) Gas chromatogram for clove. The red bars in the lower panel indicate the only three periods during which glomerular responses were observed. Blue arrows indicate the chemical structure specified by the mass spectrum at each time point. Scale bars = 1000 mV / 50 s.

(B) Intrinsic signal image from each red time point in (A). Scale bar = 200 μm. M, medial; A, anterior.

(C) Response to whole clove.

(D) Responses to pure forms of each of the three ligands identified in (A).

(E) Response to a mixture of all three ligands.

(F) Pseudocolor maps showing the overlapping activation pattern for each pure component and its corresponding GC peak. Green pixels were activated in (B), red pixels were activated in (D), and yellow pixels denote regions of overlap.

(G) Pseudocolor map showing the overlapping activation pattern for clove and the tertiary mixture; color as in (F).

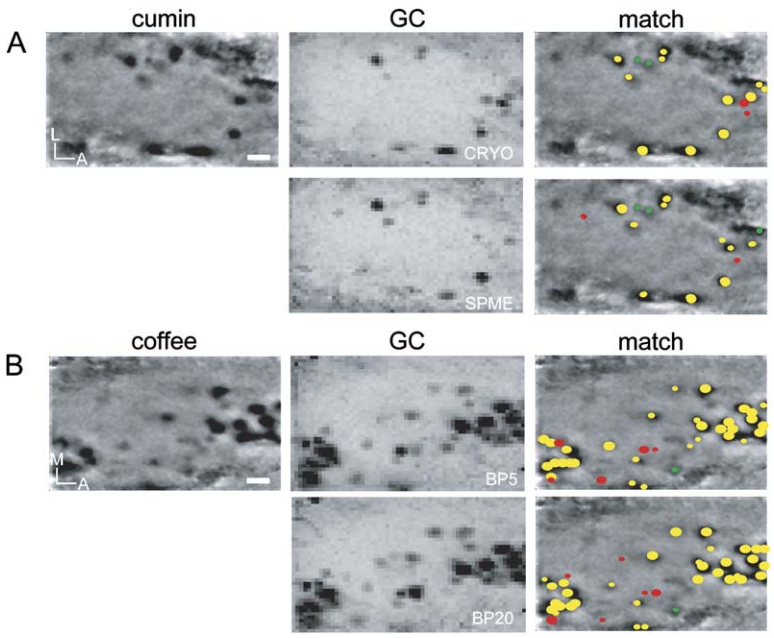

Figure 7. Cumulative Responses during GC Separation Closely Match Responses to Whole Stimuli

(A) Comparison of the response to whole cumin with the cumulative response to GC-separated cumin. The left panel shows the response to whole cumin; scale bar = 200 μm. L, lateral; A, anterior. The middle panels show the cumulative responses to GC-separated cumin using different methods for concentrating volatiles. The right panels show the match quality (see Experimental Procedures) between each GC method and the whole stimulus overlaid on the response to whole cumin. Red dots mark glomeruli activated only during GC runs and green dots indicate glomeruli only activated by whole stimuli; yellow dots mark shared glomeruli. Large dots denote Z score ≤ -3, and small dots denote $-3 < Z$ score ≤ -2. The sizes of yellow dots reflect the Z score for the glomerulus during GC presentation.

(B) Comparison of the response to whole coffee with the cumulative response to GC-separated coffee. Organized as in (A), comparing two different GC separation columns. Scale bar = 200 μm. M, medial; A, anterior.

observed with different concentrating methods or GC columns (Figure 7). Cooking or heating can change the chemical composition and odor quality of a stimulus (Koizumi et al., 1987). As the GC injection port and oven temperature needs to reach >200ºC to efficiently release and separate compounds, some heat-sensitive chemicals can be decomposed, dehydrated, or oxidized during the process.

To investigate the possibility that new compounds were generated during GC runs, we first examined the intrinsic signal images using heated (at 200ºC for 5–15 min) cumin or clove. Over ten additional glomeruli were activated with heated stimuli as compared with responses to unheated stimuli (Figure S7). Most of these glomeruli were common to both heated cumin and heated clove and appeared to cluster together in an anterior region of the MOB. Comparing GC profiles of heated and unheated clove and cumin, we identified a common group of compounds in the heated forms with low molecular mass, including 2MB, 3MB, and 2MBE, which are also enriched in roasted coffee. We next tested whether the extra glomeruli that appeared during GC runs were the same as those that were unique to heat-treated stimuli. In three experiments, 8 out of 13 strongly activated glomeruli (Z score ≤ -3) which were observed only during GC runs were matched in response maps of heat-treated stimuli (Figures 8B and 8C). We then tested whether the matching quality improved using heat-treated whole and fractionated stimuli. In four experiments using heated clove or cumin as our stimuli, the overall matching quality between two approaches showed some improvement, but this difference was not significant (matching quality = 89% ± 1.6%; unpaired t test, p = 0.10). However, the matching quality was substantially improved for strongly activated glomeruli (94%; 47/50), while the agreement between weakly activated glomeruli (80%; 66/83) was comparable to the matching quality in unheated conditions (77%). These results suggest that some of the discrepancies between whole stimulus responses and the accumulated responses to fractionated stimuli can be explained by the generation of new volatiles during the GC procedure.

Discussion

Here we report on the representation of natural odor stimuli and their fractionated molecular constituents, as assessed by intrinsic signal imaging in the MOB. While substantial evidence indicates that temporal dynamics of odor responses may contribute to coding of odor identity (Laurent, 2002), due to the relatively low temporal resolution of intrinsic signal imaging and GC, we focused solely on the principles of spatial representations.

Despite containing over 100 volatile components, natural stimuli are encoded in the MOB by a relatively small and distinct subpopulation of glomeruli, with individual components only activating one or a few visible glomeruli. Moreover, while many mixture components are represented, the glomerular units that make up the spatial pattern appear to be quite selectively tuned. Therefore, we conclude that representations of complex stimuli at their native concentrations are relatively sparse. The response pattern for a natural stimulus closely matches a linear combination of those of its individual components, suggesting that components are processed independently.

We caution that our data can only directly speak to the properties of the visible dorsal surface imaged here. Further work is required to determine whether the coding principles we observed can be generalized to other areas of the bulb. Studies that visualized more extensive odor responses have shown that certain stimulus sets tend to preferentially activate glomeruli in regions that we were unable to image (Johnson et al., 2002; Xu et al., 2003; Igarashi and Mori, 2005). It is therefore possible that functional differences among other regions of

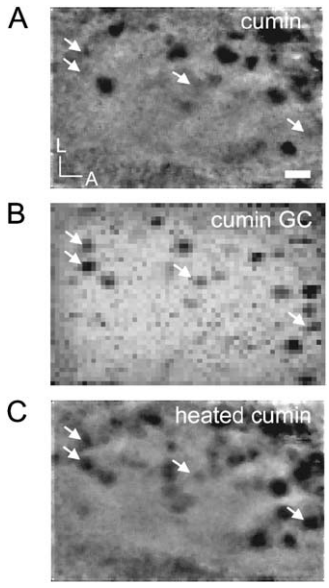

Figure 8. Many Extra Glomeruli Activated during GC Elution Are Also Activated by Heated Stimuli

(A) Response to unheated cumin. Scale bar = 200 μm.

(B) Cumulative response to GC-separated cumin.

(C) Response map to heated cumin. Arrows indicate four glomeruli activated during GC elution of cumin but not presentation of whole cumin. These glomeruli are activated during presentation of whole cumin that has been heat treated.

the bulb, including differences in receptive field size, may lead to deviation from our findings.

Sparse Natural Odorant Representation

Previous imaging studies using relatively high concentrations of monomolecular odorants found that many compounds generated widespread responses from dorsal glomeruli in the MOB (Meister and Bonhoeffer, 2001; Takahashi et al., 2004a). In contrast, despite their complexity many natural stimuli failed to elicit any responses on the visible dorsal surface area of the MOB, and others activated a relatively small but distinctive subset of glomeruli (<20%). Although intrinsic signal imaging may fail to detect some weak activity, systematic mitral cell recordings using mouse urine and other natural stimuli revealed that only 3%–10% of recorded cells were responsive for each natural stimulus by measure of firing rate (Lin et al., 2005). Thus, complex odorants at their natural concentrations are sparsely encoded by a relatively small number of active neurons. Similar sparse coding strategies are evidenced in many other sensory systems, and they have been proposed to decrease the ambiguity of natural sensory inputs and increase energy efficiency (Olshausen and Field, 2004).

There are two possible mechanisms that may underlie this apparently sparse code. One possibility is that few components in a natural stimulus are above threshold for detection and the pattern of glomeruli reflects responses to only those few components, each involving multiple glomeruli. The alternative possibility is that many chemicals contribute to the response map, with each activating a smaller number of glomeruli. Numerous GC-O studies with human subjects are consistent with the latter hypothesis, as over 20 distinct aromas can often be detected in a fractionated natural stimulus (Leland et al., 2001). Moreover, in our previous study we identified more than 30 GC peaks in mouse urine that can activate mitral cells (Lin et al., 2005). Indeed, when individual components were delivered to the animal sequentially, we observed glomerular responses at many time points, and only one or very few glomeruli (median = 1, mean = 1.2) were activated during each response. Response intensity was uncorrelated with peak size. Some peaks that are readily detectable by human observers elicited no glomerular responses, presumably due to the limited area accessible for imaging.

These sparse odor representations were observed with odors presented at their native concentrations. However, in other imaging studies, glomerular activation varied dramatically with concentration (Meister and Bonhoeffer, 2001; Fried et al., 2002). At high concentrations, odorants tend to elicit widespread activations, and the response patterns of structurally similar compounds overlap heavily (Meister and Bonhoeffer, 2001). Indeed, when we raised concentrations of 2MB, 3MB, or 2MBE from 10^{-8} to 10^{-6} (v/v), some initially inactivated glomeruli were recruited, and the response intensity of the most sensitive glomeruli increased (Figures S5A–S5C). It is unclear how odor quality can be maintained as representations expand with increasing concentration; potential solutions have been proposed involving temporal dynamics across an ensemble of neurons (Hopfield, 1995; Stopfer et al., 2003) or presynaptic gain control mechanisms (McGann et al., 2005). Nonetheless, because we used stimuli at their native concentration, the sparse odor representations observed in this study are likely reflective of the naturalistic coding of complex odorants.

Highly Specific Glomerular Response

When mitral cells were sequentially presented with individual components in mouse urine, they often responded to only one component out of hundreds (Lin et al., 2005). We have obtained similar results using the same approach with a broader panel of natural stimuli (D.Y.L. and L.C.K., unpublished data). When cells responded to multiple stimuli, it was typically due to the same component present in all of the stimuli. In the present study, we further examined the specificity of glomerular responses using intrinsic signal imaging. Seventy-two percent of glomeruli responded to only one peak during the whole GC run. This is comparable to the proportion of mitral cells activated at a single time point during GC delivery of urine (75%) (Lin et al., 2005).

This apparent specificity was not due to a lack of structurally similar compounds. In some cases, other stimulus components structurally related to the effective ligands were identified by GC-MS. The specificity also did not result from inadequate concentration during GC runs because the cumulative response matched well with the response to intact stimuli. When several glomerular responses were tested with a panel of 29 closely structurally related chemicals at their natural concentration, their sensitivity was found to be quite restricted. We therefore speculate that individual glomeruli have very limited receptive ranges under natural conditions. This is consistent with our observation that

when two distinct stimuli activate the same glomerulus, it is often due to the shared presences of the same component or two structurally similar components (Figures 5A–5D).

Superficially, this may seem to drastically limit the extent of chemical odor space that can be represented by the MOB. However, in a survey of information from a flavor database (Flavor-Base 2004, Leffingwell and Associates, Canton, GA), only 2825 chemicals are found in over 200 natural products from 3904 previous reports. If the mammalian olfactory system is designed to represent on the order of 5000 chemicals, then even highly selective glomeruli or mitral cells may sufficiently encode most of the relevant chemical space.

Largely Independent Representation of Individual Components

The GC-I technique has some limitations that may restrict our ability to observe minor interactions between components. Given the small size of the intrinsic signals relative to baseline fluctuations (0.1%), measurements of response intensity in this study could only be semiquantitative. Interactions among mixture components resulting in only subtle changes in magnitude may therefore be missed. Nevertheless, to the resolution of our technique and within the imaged region, the response to a natural stimulus closely matches the sum of the responses to its isolated components. We thus conclude that components of natural stimuli are largely processed independently, with limited interactions among their representative glomeruli.

In one experiment, we recapitulated the dorsal glomerular response patterns to clove with a mixture of three chemicals. If one could identify the set of components required to generate the clove response throughout the bulb, our data predict that this sparse mixture would be perceptually indistinguishable from the intact natural stimulus. Such an experiment would confirm that intrinsic imaging can capture all salient aspects of these odor representations. Alternatively, psychophysical data from humans regarding dominant odors in natural mixtures suggest that a synthetic blend of less than 5% of the volatiles in a food may be equivalent (Grosch, 2001).

Occasionally, we found activated glomeruli during GC runs that were not observed in response to the heat-treated form of the corresponding natural stimulus. However, the position and identity of these mismatched glomeruli usually varied between animals. These inconsistencies inhibited further investigation of the potential interactions involving the respective components.

Our current knowledge of low-level olfactory processing (including the ORs and the MOB) suggests three potential locations where interactions between mixture components can occur: (1) agonistic and antagonistic effects between ligands at the receptor level (Araneda et al., 2000; Oka et al., 2004); (2) interglomerular inhibitory interactions mediated by short axon cell contacts onto GABAergic periglomerular neurons (Aungst et al., 2003); and (3) the inhibitory network formed by reciprocal synapses between the lateral dendrites of mitral cells and the dendrites of granule cells in the MOB (Rall et al., 1966). Peripheral masking may be uncommon in light of the scarcity of demonstrable antagonists to one specific receptor (Oka et al., 2004). Pharmacological perturbations of inhibitory networks in the glomerular layer or the granule cell layer induce changes in glomerular and mitral cell activities, suggesting that interglomerular interactions indeed shape odor representations (Yokoi et al., 1995; Vucinic et al., 2005; cf. McGann et al., 2005). Center-surround structure has been observed within inhibitory networks in the MOB, but this inhibitory effect is concentration-dependent and is only observed with high concentrations of odorants (Wilson and Leon, 1987; Luo and Katz, 2001). It is unclear whether the inhibition that a glomerulus or mitral cell exerts on neighboring glomeruli is sufficient to suppress the excitatory response to another ligand under natural conditions. Alternatively, inhibitory networks may act as a spatial high pass filter (Urban, 2002) or gain control mechanism (McGann et al., 2005), eliminating nonspecific weak activation at elevated odor concentrations.

Intrinsic signals are likely to reflect activity in both OR terminals and mitral cell bodies (Wachowiak and Cohen, 2003), thus complicating estimation of the contribution of inhibitory networks to the structure of response maps. Although we cannot rule out mutual interactions among mitral cells, our unit recordings from mitral cells show no evidence that responses to a component differ when presented in mixture. Urine-responsive mitral cells showed responses to one or a few peaks eluted from the GC that were always very similar to their response to urine. MTMT, a male specific urine component, evoked identical mitral cell responses when it was presented alone or in the urine background (Lin et al., 2005). Therefore, the available evidence from our imaging and electrophysiology studies suggests that the reshaping of neural activity by interactions among individual components is limited and unlikely to dramatically affect the representation of the complete natural stimulus.

Human psychophysical studies demonstrate that mixed odorants can induce a percept that is distinct from a simple superposition of the component scents (Jinks and Laing, 2001). Thus, while at the level of the MOB individual odorants may be encoded independently, synthetic processing must occur in higher brain areas through mechanisms that remain to be elucidated.

Experimental Procedures

Animal Preparation

GC-I experiments were performed on 32 female Balb/C mice (8–16 weeks old). Mice were initially anesthetized with a mixture of ketamine (200 mg/kg, i.p.) and xylazine (10 mg/kg, i.p.), and allowed to breathe freely; anesthesia was maintained with isofluorane (1%–3%). Once anesthetized, animals were placed in a stereotaxic apparatus and the bone overlying the dorsal surface of one olfactory bulb was thinned for imaging as described previously (Rubin and Katz, 1999). All mice used in this study were maintained in strict accordance with National Institutes of Health and institutional animal care guidelines.

Intrinsic Signal Imaging

Intrinsic signals were recorded using a commercially available imaging system (Imager 2001, Optical Imaging Inc., Mountainside, NJ). Before each experiment, the surface blood vessel pattern was acquired under green light illumination (546 nm). Light reflectance from the surface of the OB (630 nm wavelength light illumination) was captured using a CCD camera (XC-ST70, Sony, New York City, NY), digitized, and acquired to a computer hard disk using a frame grabber board (Matrox Genesis, Droval, Quebec, Canada).

We imaged a 2.1 × 1.65 mm region with a spatial resolution of 372 × 240 pixels (after 2 × 2 binning), which contains about 10% of the 1800 glomeruli in one bulb (Royet et al., 1988). For each imaging trial using the whole odor stimulus, data were collected for 60 s with a frame duration of 1 s. Odorant stimulation was applied from the beginning of the fourth to the end of the ninth frame (6 s). Stimuli were tested at least three times. For recording trials using GC delivery, images were collected continuously at a rate of 1 frame/s during GC runs. Due to the limitations of our imaging system, in order to maintain a stable image, the data collection was suspended for 10 s once every 70 s to acquire a new reference image. The timing of these references images relative to GC elution was shifted in consecutive trials to allow offline reconstruction of a continuous image set. Each reconstructed GC image set included at least three individual trials.

Odor Stimuli

Mouse urine was collected as described (Lin et al., 2005). Bobcat and red fox urine were a kind gift from Dr. Bill Graham and Dr. Dan Warczok (Leg Up Enterprises, Lovell, ME); urine was freshly collected, shipped on dry ice and stored at −80ºC until use. All other stimuli were purchased from local stores. Three grams of each dry solid stimulus was placed in 40 ml vials. For liquid stimuli, such as fox and bobcat urines, 2 ml of each were used. For mouse urine, 300 μl each of Balb/C ♂, Balb/C ♀, C57BL/6 ♂, and C57BL/6 ♀ were pooled into each vial. A 64 channel olfactometer was used to deliver volatiles from those vials to the nose at a rate of 4 ml/s for 6 s.

Volatile compounds from each natural stimulus (clove, coffee, and cumin) were separated with GC (Model 6890, Agilent, Palo Alto, CA). This technique, though powerful, has some technical limitations including inherent biases in volatile concentration methods and modification of some compounds by the GC process. We have tried to address both issues with our approach (see text) (van Ruth, 2001). Two independent concentrating methods are used. For the SPME method, an SPME fiber (2 cm to 50/30 μm DVD/Carboxen/PDMS StableFlex, Supelco, Central Hall, PA) was inserted into the headspace of an olfactometer vial for 30–60 s. The fiber was then retracted from the vial and inserted into the GC injection port, immediately desorbing the extracted volatiles at 260ºC for 3 min. Either a nonpolar BP-5 or a polar BP-20 column (both 30 m × 0.53 mm i. d.; film thickness = 1 μm; SGE) was used to achieve chemical separation. Dynamic on-column cryotrapping locally cools a short piece of column immediately adjacent to the GC injection port, condensing any gas phase volatiles. For this method, the guard column (BP-5, 0.53 mm i. d.; film thickness = 1 μm) was first cooled to −70ºC using an on-column 4 inch cryotrap system (SIS. Inc, Ringoes, NJ) with liquid CO_2. Then, the headspace of an olfactometer vial was slowly purged into the injection port at a rate of 6 ml/min for 2–3 min and condensed in the guard column. One minute after the completion of the injection, the guard column was heated to 250ºC at a rate of 400ºC/min to release all condensed compounds into the BP-5 column. The carrier gas was helium (flow 6 ml/min).

Cumin and clove volatiles were separated in an oven maintained at 60ºC for 2 min, then heated at a rate of 15ºC/min to 260ºC and maintained for 1 min. Because coffee contains mainly low molecular mass compounds, a lower initial GC temperature was used to achieve better separation. The column was held at 40ºC for 1 min and raised to 120ºC at a rate of 10ºC/min, then further ramped to 200ºC at 20ºC/min. In all GC conditions, half of the effluent from the column was routed to either an FID (Agilent, Palo Alto, CA) or MSD (Model 5973, Agilent, Palo Alto, CA); the other half was delivered to the nose via a heated transfer line (Microanalytics, Round Rock, TX). The FID and MSD operation conditions were identical to those in our previous study (Lin et al., 2005).

Calculation of Response Maps for Whole Stimuli

All raw imaging data were initially visualized using Winmix 1.9 (Optical Imaging, Inc., Mountainside, NJ). Using custom MatLab (MathWorks, Natick, MA) software, each frame was read into a two-dimensional matrix containing the position and intensity value for each pixel. To obtain responses for whole odor stimuli, adjacent pixels in individual frames were binned to a final resolution of 186 × 120. Signals recorded during odor stimulation (t = 4–9 s) were then averaged across trials, and a baseline image (t = 3 s) was subtracted. In some cases, signals obtained after odor offset (t = 25–29 s) were also included in the generation of the final image to visualize the activities of slow responding glomeruli (Figure S1A). Frames were low-pass filtered by convolution with a 2D Gaussian kernel (30 pixels half width), and the result was subtracted from the raw image to eliminate diffuse activation (Meister and Bonhoeffer, 2001). To quantify the signal intensity, a Z score was calculated for each pixel as follows: Z = (pixel intensity - mean intensity for all pixels in the frame)/(adjusted standard deviation). Adjusted standard deviation (SD) was the SD value obtained from all pixels in the frame excluding those >2 SD from the mean. We observed that those pixels frequently corresponded to activated glomeruli, intact bone, and major blood vessels; thus, including them would result in overestimation of the noise level. Glomeruli with Z scores ≤ -3 at their center were regarded as strongly activated and those with Z scores between −3 and −2 were regarded as weakly activated.

Using individual odor responses, a composite map (Figure 1N) was calculated as follows. Each pixel from a single odor map was compared with the corresponding pixel in other single odor maps for Z score value. The value of lowest Z score (highest activity) was assigned to each pixel in the composite map.

To quantify the time course of a glomerular response, all pixels in a response map were clustered using a MatLab program with each cluster representing an activated glomerulus. A baseline prestimulus frame was subtracted from each frame between 4 and 60 s to produce a series of images showing signal changes from the background. The response of each glomerulus in time was calculated by plotting the mean value of all pixels in the cluster for each frame in the series.

Identification of Glomerular Responses during GC Runs

Frames recorded during GC runs were binned at 40 × 62 to ease computational load while retaining adequate spatial resolution to distinguish a glomerulus (usually an oval with a diameter 3–6 pixels at this resolution). In this continuous acquisition mode, frame(n)′ = frame(n) − frame(n – 10). Sets of processed images obtained under the same GC condition were averaged using GC signal peaks for alignment. Custom programs written in MatLab were then used to identify activated glomeruli in those reconstructed images by comparing the value of each pixel and its surroundings. In detail, a pixel was regarded as activated if it met three criteria. First, its intensity was 2 SD lower than that of the surrounding area, with surrounding area defined as a ring three pixels wide with an inner radius of four pixels. Second, the same pixel met the first criterion in five continuous frames. Third, at least one adjacent pixel also met the first two criteria. Once all activated pixels were defined in every frame, they were clustered together according to their location in space and time. Each spatiotemporal cluster was identified as an activated glomerulus. Visual inspection was also used to verify the expected glomerular shape and prevent false positives (e.g., pixels at the edge or in bony areas). For each glomerulus detected during the GC run, we then obtained a single representative frame by averaging all frames containing the activated glomerulus (or the first ten frames if the activation lasted longer than 10 s). The Z score of each activation was calculated as follows: Z score = (intensity of the activated pixel - averaged intensity of the whole imaging area)/adjusted SD. Glomeruli with Z scores below −3 were considered to be strongly activated.

Comparing Whole Stimulus and Cumulative GC Responses

In order to compare responses during GC runs with the response to an intact stimulus, a cumulative response was constructed from all processed frames in a GC run. In detail, for each pixel, intensity was plotted as a function of time over the whole GC run. After smoothing this function with a 6 s boxcar window, its minimal value was applied to that pixel in the cumulative response.

To quantify the agreement between glomerular activation patterns during GC runs and patterns elicited by the intact stimulus, each glomerulus determined to be active during GC runs was compared with the corresponding region of the whole stimulus response. If the center of a glomerulus activated during a GC run was aligned with an activated area (Z score ≤ -2) in the whole stimulus response, the glomerulus was deemed to be matched. If a glomerulus was activated multiple times during a GC run, only the activation with the lowest Z score (strongest activation) was considered when calculating the

matching quality. A glomerulus that was either present only during the GC run or present only in the whole stimulus response was considered unmatched. Matching quality = Σ [(matchglom$_i$) (w_i)]/Σ (allglom$_i$) (w_i). Allglom denotes all glomeruli in either or both responses, while matchglom corresponds to only glomeruli in both stimuli. A glomerulus with Z score ≤ -3 was assigned a glomerular weight (w) of 2. Otherwise, the glomerular weight was 1.

Supplemental Data

The Supplemental Data for this article can be found online at http://www.neuron.org/cgi/content/full/50/6/937/DC1/.

Acknowledgments

We are grateful to David Fitzpatrick, Ian Davison, and Richard Mooney for helpful discussions and comments regarding earlier versions of the manuscript. This work was supported by the NIH DC005671 to L.C.K., and a predoctoral fellowship to D.Y.L. from the Ruth K. Broad Biomedical Research Foundation. L.C.K. was also an Investigator in the Howard Hughes Medical Institute. We dedicate this paper to the fond memory of our mentor and friend Dr. Lawrence C. Katz.

Received: January 26, 2006
Revised: March 9, 2006
Accepted: March 16, 2006
Published: June 14, 2006

References

Araneda, R.C., Kini, A.D., and Firestein, S. (2000). The molecular receptive range of an odorant receptor. Nat. Neurosci. *3*, 1248–1255.

Aungst, J.L., Heyward, P.M., Puche, A.C., Karnup, S.V., Hayar, A., Szabo, G., and Shipley, M.T. (2003). Centre-surround inhibition among olfactory bulb glomeruli. Nature *426*, 623–629.

Belluscio, L., and Katz, L.C. (2001). Symmetry, stereotypy, and topography of odorant representations in mouse olfactory bulbs. J. Neurosci. *21*, 2113–2122.

Bozza, T., Feinstein, P., Zheng, C., and Mombaerts, P. (2002). Odorant receptor expression defines functional units in the mouse olfactory system. J. Neurosci. *22*, 3033–3043.

Bozza, T., McGann, J.P., Mombaerts, P., and Wachowiak, M. (2004). In vivo imaging of neuronal activity by targeted expression of a genetically encoded probe in the mouse. Neuron *42*, 9–21.

Buck, L., and Axel, R. (1991). A novel multigene family may encode odorant receptors: a molecular basis for odor recognition. Cell *65*, 175–187.

Fried, H.U., Fuss, S.H., and Korsching, S.I. (2002). Selective imaging of presynaptic activity in the mouse olfactory bulb shows concentration and structure dependence of odor responses in identified glomeruli. Proc. Natl. Acad. Sci. USA *99*, 3222–3227.

Grosch, W. (2001). Evaluation of the key odorants of foods by dilution experiments, aroma models and omission. Chem. Senses *26*, 533–545.

Guthrie, K.M., Anderson, A.J., Leon, M., and Gall, C. (1993). Odor-induced increases in c-fos mRNA expression reveal an anatomical "unit" for odor processing in olfactory bulb. Proc. Natl. Acad. Sci. USA *90*, 3329–3333.

Hopfield, J.J. (1995). Pattern recognition computation using action potential timing for stimulus representation. Nature *376*, 33–36.

Igarashi, K.M., and Mori, K. (2005). Spatial representation of hydrocarbon odorants in the ventrolateral zones of the rat olfactory bulb. J. Neurophysiol. *93*, 1007–1019.

Jinks, A., and Laing, D.G. (2001). The analysis of odor mixtures by humans: evidence for a configurational process. Physiol. Behav. *72*, 51–63.

Johnson, B.A., Ho, S.L., Xu, Z., Yihan, J.S., Yip, S., Hingco, E.E., and Leon, M. (2002). Functional mapping of the rat olfactory bulb using diverse odorants reveals modular responses to functional groups and hydrocarbon structural features. J. Comp. Neurol. *449*, 180–194.

Koizumi, Y., Nagashima, T., Yamada, M., and Yanagida, F. (1987). Curry. V. Changes of aroma components during processing of commercial cooked curry. Nippon Shokuhin Kogyo Gakkaishi *34*, 244–248.

Laurent, G. (2002). Olfactory network dynamics and the coding of multidimensional signals. Nat. Rev. Neurosci. *3*, 884–895.

Leland, J.V., Schieberle, P., Buettner, A., and Acree, T.A. (2001). Gas Chromatography-Olfactometry: The State of the Art (Washington, DC: Oxford University Press).

Lin, D.Y., Zhang, S.Z., Block, E., and Katz, L.C. (2005). Encoding social signals in the mouse main olfactory bulb. Nature *434*, 470–477.

Luo, M., and Katz, L.C. (2001). Response correlation maps of neurons in the mammalian olfactory bulb. Neuron *32*, 1165–1179.

McGann, J.P., Pirez, N., Gainey, M.A., Muratore, C., Elias, A.S., and Wachowiak, M. (2005). Odorant representations are modulated by intra- but not interglomerular presynaptic inhibition of olfactory sensory neurons. Neuron *48*, 1039–1053.

Meister, M., and Bonhoeffer, T. (2001). Tuning and topography in an odor map on the rat olfactory bulb. J. Neurosci. *21*, 1351–1360.

Mombaerts, P., Wang, F., Dulac, C., Chao, S.K., Nemes, A., Mendelsohn, M., Edmondson, J., and Axel, R. (1996). Visualizing an olfactory sensory map. Cell *87*, 675–686.

Oka, Y., Omura, M., Kataoka, H., and Touhara, K. (2004). Olfactory receptor antagonism between odorants. EMBO J. *23*, 120–126.

Olshausen, B.A., and Field, D.J. (2004). Sparse coding of sensory inputs. Curr. Opin. Neurobiol. *14*, 481–487.

Rall, W., Shepherd, G.M., Reese, T.S., and Brightman, M.W. (1966). Dendrodendritic synaptic pathway for inhibition in the olfactory bulb. Exp. Neurol. *14*, 44–56.

Roberts, D.D., Pollien, P., and Milo, C. (2000). Solid-phase microextraction method development for headspace analysis of volatile flavor compounds. J. Agric. Food Chem. *48*, 2430–2437.

Royet, J.P., Souchier, C., Jourdan, F., and Ploye, H. (1988). Morphometric study of the glomerular population in the mouse olfactory bulb: numerical density and size distribution along the rostrocaudal axis. J. Comp. Neurol. *270*, 559–568.

Rubin, B.D., and Katz, L.C. (1999). Optical imaging of odorant representations in the mammalian olfactory bulb. Neuron *23*, 499–511.

Schaefer, M.L., Young, D.A., and Restrepo, D. (2001). Olfactory fingerprints for major histocompatibility complex-determined body odors. J. Neurosci. *21*, 2481–2487.

Spors, H., and Grinvald, A. (2002). Spatio-temporal dynamics of odor representations in the mammalian olfactory bulb. Neuron *34*, 301–315.

Stopfer, M., Jayaraman, V., and Laurent, G. (2003). Intensity versus identity coding in an olfactory system. Neuron *39*, 991–1004.

Tabor, R., Yaksi, E., Weislogel, J.M., and Friedrich, R.W. (2004). Processing of odor mixtures in the zebrafish olfactory bulb. J. Neurosci. *24*, 6611–6620.

Takahashi, Y.K., Kurosaki, M., Hirono, S., and Mori, K. (2004a). Topographic representation of odorant molecular features in the rat olfactory bulb. J. Neurophysiol. *92*, 2413–2427.

Takahashi, Y.K., Nagayama, S., and Mori, K. (2004b). Detection and masking of spoiled food smells by odor maps in the olfactory bulb. J. Neurosci. *24*, 8690–8694.

Tassan, C.G., and Russell, G.F. (1975). Chemical and sensory studies on cumin. J. Food Sci. *40*, 1185–1188.

Uchida, N., Takahashi, Y.K., Tanifuji, M., and Mori, K. (2000). Odor maps in the mammalian olfactory bulb: domain organization and odorant structural features. Nat. Neurosci. *3*, 1035–1043.

Urban, N.N. (2002). Lateral inhibition in the olfactory bulb and in olfaction. Physiol. Behav. *77*, 607–612.

van Ruth, S.M. (2001). Methods for gas chromatography-olfactometry: a review. Biomol. Eng. *17*, 121–128.

Vucinic, D., Cohen, L.B., and Kosmidis, E.K. (2005). Interglomerular center-surround inhibition shapes odorant-evoked input to the mouse olfactory bulb in vivo. J. Neurophysiol. *95*, 1881–1887.

Wachowiak, M., and Cohen, L.B. (2001). Representation of odorants by receptor neuron input to the mouse olfactory bulb. Neuron *32*, 723–735.

Wachowiak, M., and Cohen, L.B. (2003). Correspondence between odorant-evoked patterns of receptor neuron input and intrinsic optical signals in the mouse olfactory bulb. J. Neurophysiol. *89*, 1623–1639.

Wachowiak, M., Denk, W., and Friedrich, R.W. (2004). Functional organization of sensory input to the olfactory bulb glomerulus analyzed by two-photon calcium imaging. Proc. Natl. Acad. Sci. USA *101*, 9097–9102.

Wilson, D.A., and Leon, M. (1987). Evidence of lateral synaptic interactions in olfactory bulb output cell responses to odors. Brain Res. *417*, 175–180.

Xu, F., Liu, N., Kida, I., Rothman, D.L., Hyder, F., and Shepherd, G.M. (2003). Odor maps of aldehydes and esters revealed by functional MRI in the glomerular layer of the mouse olfactory bulb. Proc. Natl. Acad. Sci. USA *100*, 11029–11034.

Yang, X., Renken, R., Hyder, F., Siddeek, M., Greer, C.A., Shepherd, G.M., and Shulman, R.G. (1998). Dynamic mapping at the laminar level of odor-elicited responses in rat olfactory bulb by functional MRI. Proc. Natl. Acad. Sci. USA *95*, 7715–7720.

Yokoi, M., Mori, K., and Nakanishi, S. (1995). Refinement of odor molecule tuning by dendrodendritic synaptic inhibition in the olfactory bulb. Proc. Natl. Acad. Sci. USA *92*, 3371–3375.